Organic & Biomolecular Chemistry

PAPER

View Article Online
View Journal

Cite this: DOI: 10.1039/c5ob02625c

Synthesis and SAR assessment of novel Tubathian analogs in the pursuit of potent and selective HDAC6 inhibitors†

Rob De Vreese,[a] Yves Depetter,[a] Tom Verhaeghe,[b] Tom Desmet,[b] Veronick Benoy,[c] Wanda Haeck,[c] Ludo Van Den Bosch[c] and Matthias D'hooghe*[a]

Received 21st December 2015,
Accepted 5th January 2016

DOI: 10.1039/c5ob02625c

www.rsc.org/obc

The synthesis of novel isoform-selective HDAC inhibitors is considered to be an important, emerging field in medicinal chemistry. In this paper, the preparation and assessment of thirteen selective HDAC6 inhibitors is disclosed, elaborating on a previously developed thiaheterocyclic Tubathian series. All compounds were evaluated *in vitro* for their ability to inhibit HDAC6, and a selection of five potent compounds was further screened toward all HDAC isoforms (HDAC1-11). The capability of these Tubathian analogs to inhibit α-tubulin deacetylation was assessed as well, and ADME/Tox data were collected. This thorough SAR evaluation revealed that the oxidized, *para*-substituted hydroxamic acids can be recognized as valuable lead structures in the pursuit of novel potent and selective HDAC6 inhibitors.

Introduction

The interplay between histone acetyltransferases (HATs) and histone deacetylases (HDACs) represents an important epigenetic regulatory mechanism in the biochemistry of life processes.[1] This epigenetic interaction controls the structural transformation of DNA between a compact, inactivated form and a loosely bound, activated form, and thus plays a major role in the functioning of cells.[2] Besides the regulation of histone acetylation, HATs and HDACs mediate the acetylation of other proteins as well, and therefore these enzymes are more correctly referred to as lysine acetyltransferases (KATs) and deacetylases (KDACs).[3] The KDAC family can be divided into four classes (I, IIa/IIb, III and IV), existing of 18 proteins.[4] Selective inhibition of these isoforms could significantly contribute to our knowledge on this family of epigenetic erasers (enzymes known to catalyze the removal of epigenetic marks), and potentially lead to new drugs. One of these proteins, defined as HDAC6, emerged in recent years as a valuable target in drug design and belongs to the class IIb HDACs. Because of its cytoplasmic location, HDAC6 has many interaction partners other than histones, and this feature renders it an interesting protein to study the acetylation status of proteins in cells.[3] The use of small molecule inhibitors of HDAC6 has been proposed as an efficient strategy to block its catalytic activity, and is therefore considered to be a valuable new approach in neurodegenerative diseases,[5] cancer[6] and immunology research.[7]

A milestone achievement in the quest for selective HDAC6 inhibitors concerned the development of Tubastatin A (**1**) in 2010, a molecule with a good 'drug-likeness' profile that showed great promise *in vitro* and *in vivo*.[8] This discovery, together with the growing interest of academia and industry in the design of small molecule inhibitors, prompted us to pursue new analogs of this lead compound with possibly enhanced pharmacological properties. Based on available structure–activity relationships (SAR), sulfur analogs **2** of Tubastatin A (**1**) were constructed recently by our group, as shown in Fig. 1, and tested for their ability to inhibit HDAC6 *in vitro*.[9] Within this thiaheterocyclic series, sulfone derivatives **2c** and **2d** – designated as Tubathians – exhibited the most pronounced activity and selectivity toward HDAC6.

The first major objective of the present study comprised a full and thorough biological evaluation of this Tubathian family **2** to shed more light on their potential as lead structures for HDAC6 inhibitor design. Furthermore, in view of the promising preliminary results of these Tubathian molecules, an expansion of compound library **2** to general structures **3** was envisioned as a second major objective to study structure–activity relationships in more detail. Guided by in-house docking studies and by the advancing progress made in the literature with regard to selective HDAC6 inhibitor development,[10] three main structural modifications of template mole-

[a]*SynBioC Research Group, Faculty of Bioscience Engineering, Ghent University, Coupure Links 653, B-9000 Ghent, Belgium. E-mail: matthias.dhooghe@UGent.be*
[b]*Centre for Industrial Biotechnology and Biocatalysis, Faculty of Bioscience Engineering, Ghent University, Coupure Links 653, B-9000 Ghent, Belgium*
[c]*Laboratory of Neurobiology and Vesalius Research Center (VIB), Research Institute for Neuroscience and Disease (LIND), KU Leuven, Belgium*

†Electronic supplementary information (ESI) available. See DOI: 10.1039/c5ob02625c

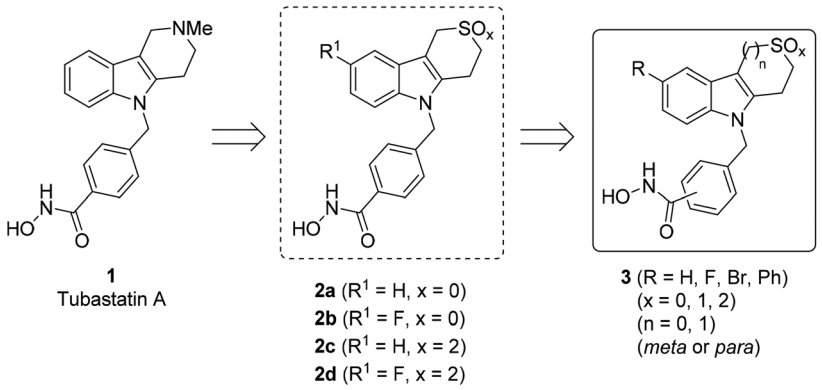

Fig. 1 Expanded SAR of sulfur analogs of Tubastatin A (**1**).

cules **2** were proposed. First, modification of the ring size of the non-aromatic C-ring (a six-membered *versus* a five-membered thiaheterocyclic ring) was pursued. A second key modification of the core scaffold molecule comprised assessment of the oxidation state of the sulfur atom, implying the selective synthesis of sulfides, sulfoxides and sulfones. Recently, also *meta*-substituted benzohydroxamic acids have been studied and showed dual HDAC6/8 selectivity.[11] Hence, the third structural variation involved the synthesis and evaluation of the *meta*-substituted counterparts of the Tubathian core structure. Once in hand, this set of compounds **2** and **3** will then be subjected to an elaborate biological investigation of their medicinal relevance as potential efficient and selective HDAC6 inhibitors.

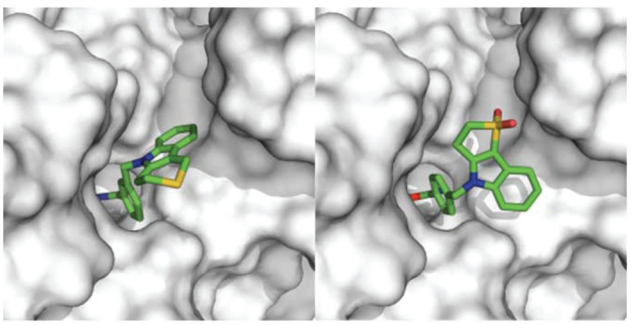

Fig. 2 Docking of selected molecules from class **3** (left: **3a**; right: **3l**) in a homology model of HDAC6 (green: carbon, blue: nitrogen, red: oxygen, yellow: sulfur).

Results and discussion

In silico docking studies of the proposed compounds **3** using a homology model of HDAC6 revealed that all theoretical structures fit the binding pocket quite well and thus represent compounds worth to be studied (Fig. 2). In general, the sulfone derivatives proved to have slightly higher predicted binding energies (better binding) than the corresponding sulfides, due to additional interactions of the sulfone group with surrounding residues. The *para*-substituted compounds resulted in better binding energies than the *meta*-substituted ones, and phenyl substitution (R = Ph) on the aromatic ring seemed to be preferred because of π-stacking interactions with the side chain of a phenylalanine amino acid. However, it must be emphasized that the differences in calculated binding energies of these virtual complexes were small, pointing to the necessity of lab synthesis and detailed biological evaluation *in vitro* (for more details on these docking studies, see ESI†).

The synthesis of compounds **2** has been reported before by us, and the same approach was used here for the preparation of molecules **3** (Scheme 1 and Fig. 3).[9] First, the tricyclic indole-containing 'cap'-group was synthesized *via* a bismuth-nitrate catalyzed Fisher-indole synthesis between aromatic hydrazines **4** and sulfur-containing cyclic ketones **5**.[12] The obtained tricycles **6** were modified through selective oxidation of the sulfur atom employing *meta*-chloroperbenzoic acid, with or without the addition of boron trifluoride, leading to the corresponding sulfoxides **7** and sulfones **8**, respectively.

7-Bromo-2,3-dihydrothieno[3,2-*b*]indole **6f** (R = Br, n = 0) appeared hard to purify because it contained the corresponding sulfoxide as a side product, which could not be removed by means of column chromatography. Therefore, this compound was used as an intermediate toward direct sulfoxidation, resulting in the synthesis of sulfoxide **7c** (R = Br, n = 0). Phenyl-containing sulfone **8f** (R = Ph, n = 1) was obtained through full oxidation of sulfide **6c** (R = Br, n = 1) to sulfone **8c** (R = Br, n = 1), followed by a Suzuki–Miyaura cross coupling. The obtained thiaheterocycles **6**, **7** and **8** were *N*-deprotonated with sodium hydride and the resulting anion subsequently quenched with methyl 4-(bromomethyl)benzoate or methyl 3-(bromomethyl)benzoate **9** to give methyl esters **10**. In the final step, esters **10** were converted to hydroxamic acids **3** upon treatment with a large excess of hydroxyl amine, which were subsequently used for pharmacological evaluation.

As can be seen from Fig. 3, no five-membered cyclic thioether-containing hydroxamic acids (with n = 0 and x = 0) were obtained, which was due to the fact that reaction of compound **6d** (R = H, n = 0) with sodium hydride and methyl 3-

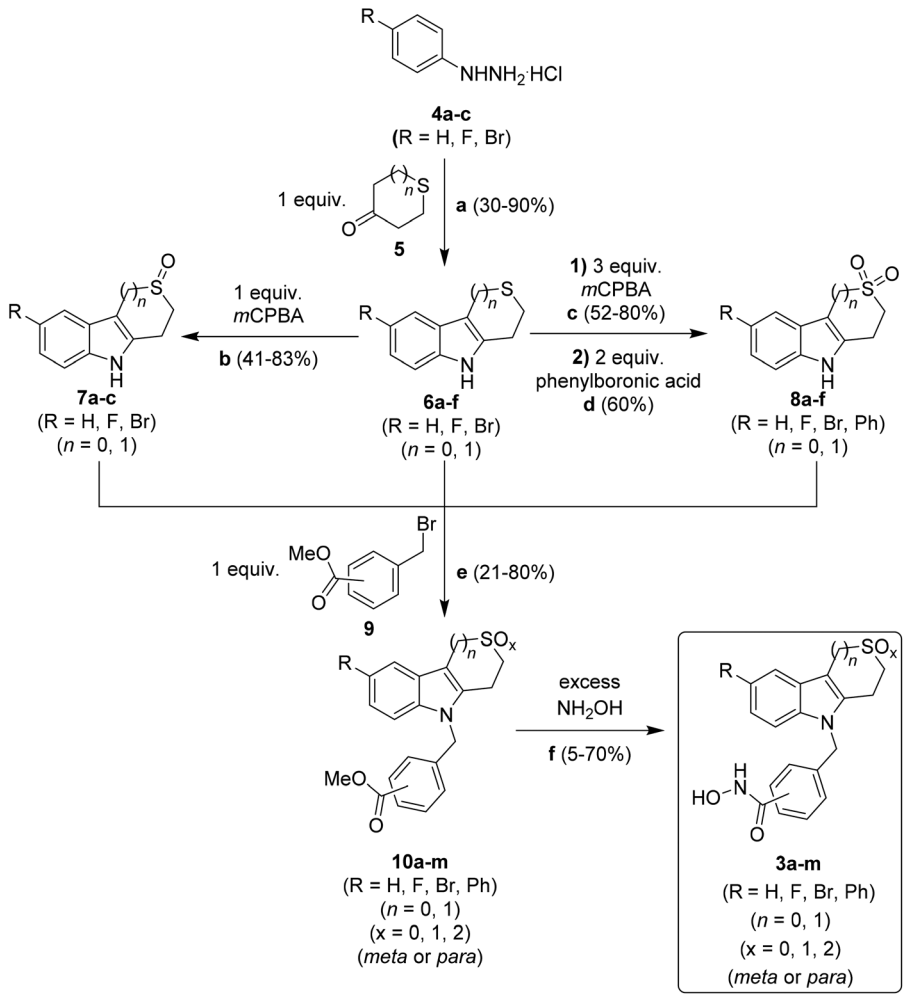

Scheme 1 Synthesis of the expanded Tubathian library **3**. Conditions: a: 1 equiv. ketone **5**, 0.2 equiv. $Bi(NO_3)_3{\cdot}5H_2O$, MeOH, Δ, 3.5 h (30–90%, **6a–f**). b: 1 equiv. *m*CPBA (≤77%), 4 equiv. $BF_3{\cdot}O(C_2H_5)_2$, THF, −20 °C, N_2, 2 h (41–83%, **7a–c**). c: 3 equiv. *m*CPBA (≤77%), THF, 0 °C to rt, 2 h (52–80%, **8a–e**). d: 2 equiv. phenylboronic acid, Na_2CO_3 (7 equiv.), 0.04 equiv. $Pd(PPh_3)_4$, toluene/ethanol/H_2O (2/1/1), Δ, N_2, 8 h (60%, **8f**). e: (1) 1 equiv. NaH, DMF, rt, N_2, 0.5 h (2) 1 equiv. methyl (bromomethyl)benzoate **9**, 0.01 equiv. KI, DMF, 80 °C, N_2, 2 h (21–80%, **10a–m**). f: 100 equiv. NH_2OH (50% in H_2O), 50 equiv. KOH (4 M in MeOH), THF, rt or Δ, 10 min (5–70%, **3a–m**).

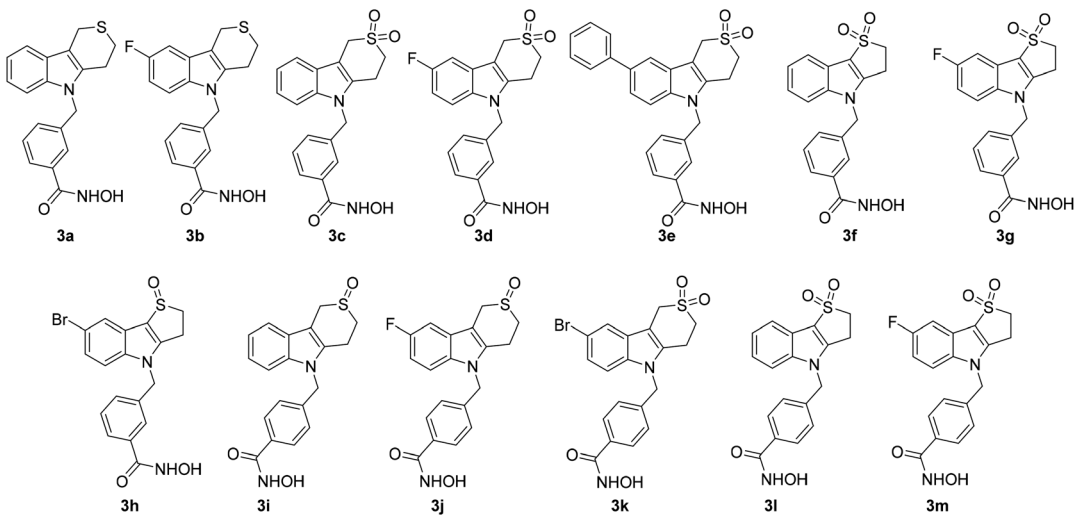

Fig. 3 Overview of the newly synthesized hydroxamic acids **3**.

(bromomethyl)benzoate or methyl 4-(bromomethyl)benzoate always resulted in complex reaction mixtures. To circumvent this problem, an alternative approach toward the synthesis of these molecules was attempted, in which the synthesis of the 'cap'-group was postponed to a later stage in the reaction pathway, however without any success.[13] In total, a set of thirteen novel hydroxamic acids **3a–m** was prepared and, together with the four earlier discovered Tubathian HDAC6 inhibitors **2a–d**, evaluated for their ability to selectively inhibit HDAC6.

A preliminary *in vitro* screening of their inhibitory potential toward HDAC6 at a concentration of 10 μM learned that the *meta*-substituted compounds **3a–h** only moderately inhibited HDAC6 (34–74% inhibition, relative to the control; see ESI† for data). This stands in sharp contrast to all the *para*-substituted compounds **2a–d** and **3i–m**, as these molecules completely inhibited HDAC6 at this concentration (99–100% inhibition, relative to the control; see ESI† for data). It must be noted that within the *meta*-substituted series, phenyl-decorated compound **3e** showed the highest inhibition percentage (74%), as predicted by the docking studies. Subsequently, the IC_{50}-values of the five new *para*-substituted compounds **3i–m** were determined and compared with the previously obtained results for compounds **2a–d** (Table 1).[9] All molecules exhibited low nanomolar IC_{50}-values toward HDAC6 (≤22 nM), and the 6-membered sulfones **2c**, **2d** and **3k** displayed the highest HDAC6 inhibitory activity (1.9, 3.7 and 3.4 nM, respectively). As noted in our previous communication,[9] this could be explained (and confirmed *in silico*) through hydrogen bond formation of both oxygen atoms on the sulfone moiety with surrounding residues.

The selectivity toward HDAC6 was assessed on the enzymatic level through a full-panel HDAC1-11 screening of representative compounds **2b**, **2c**, **2d**, **3j** and **3l**. Compounds **2b**, **2d** and **3j** were selected to compare the influence of the oxidation state of sulfur (R_2S, R_2SO and R_2SO_2) on the selectivity. The influence of the ring size (thiolane *vs.* thiane) on the inhibitory selectivity was studied by selection of hydroxamic acids **2c** and **3l**. The data in Table 2 reveal that all screened compounds display a similar selectivity profile. These molecular entities inhibit HDAC1, 2, 3, 10 and 11 at IC_{50}-values higher than 5 μM, except for the five-membered sulfone **3j**, which also shows a reasonable affinity for HDAC11 (IC_{50} = 0.52 μM). All compounds inhibit HDAC4, 5 and 8 with IC_{50}-values around 1 μM, and HDAC7 and 9 at IC_{50}-values between 0.1 and 1 μM. In all cases, the lowest values can be observed with respect to HDAC6 inhibition, with IC_{50}-values <30 nM. After this in-depth selectivity screening, it can be stated that this set of Tubathian and related compounds selectively inhibit HDAC6 in a potent and pronounced way, but also display some moderate affinity for class IIa HDACs (HDAC4, 5, 7 and 9) and HDAC8.

Table 1 *In vitro* enzyme inhibition data: IC_{50}-values toward HDAC6

Compound	**2a**	**2b**	**2c**	**2d**	**3i**	**3j**	**3k**	**3l**	**3m**
HDAC6 IC_{50} (nM)	15	22	1.9	3.7	14	9.4	3.4	8.2	16

Table 2 HDAC1-11 screening of selected compounds **2b**, **2c**, **2d**, **3j** and **3l** (IC_{50}-values in μM)[a,b]

Compound	HDAC1	HDAC2	HDAC3	HDAC4	HDAC5	HDAC6	HDAC7	HDAC8	HDAC9	HDAC10	HDAC11
2b	21	NC	23	1.5	1.8	**0.0220**	0.2	2.8	0.8	21	9.7
2c	11	26	29	1.6	0.5	**0.0019**	0.1	1.7	0.3	7.7	NC
2d	12	29	26	1.9	0.5	**0.0037**	0.1	0.9	0.5	5.9	NC
3j	9.4	>30	24	1.2	1.3	**0.0094**	0.2	2.4	0.5	6.4	0.5
3l	12	>30	NC	0.6	0.4	**0.0082**	0.1	1.9	0.2	13	17

[a] Reference compound: Trichostatin A (HDAC6 IC_{50} = 0.0093 μM). [b] Tubastatin A HDAC6 inhibition IC_{50} = 0.015 μM.[8a.] NC: IC_{50}-value not calculable. Concentration-response curve shows less than 25% effect at the highest validated testing concentration (30 μM). >30: IC_{50} value above the highest test concentration. Concentration-response curve shows less than 50% effect at the highest validated testing concentration (30 μM).

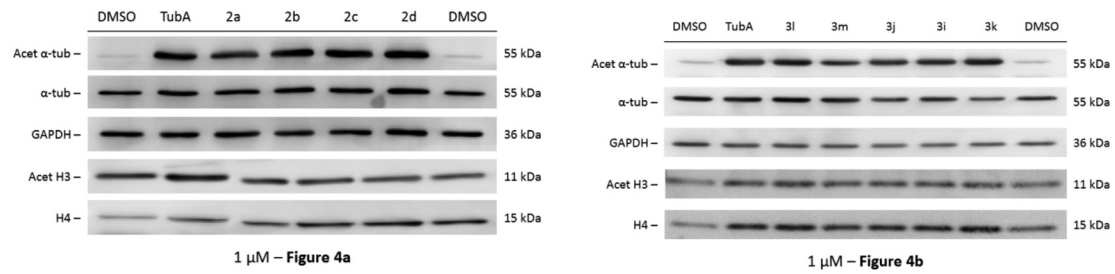

Fig. 4 (a and b) Comparison of α-tubulin and histone hyperacetylation of compounds **2a–d**, **3i–m** and control substance Tubastatin A (Neuro-2a cells, 1 μM).

Next, the potency and selectivity of compounds **2a–d**, **3i–m** together with control substance Tubastatin A was evaluated on a cellular level (Neuro-2a cells) by determining their ability to modify the acetylation level of α-tubulin (a specific HDAC6 substrate) and histones *via* western blots. First, all the compounds were tested at 1 μM for both assays. From Fig. 4 it can be seen that the HDAC6 inhibitors clearly hyperacetylate α-tubulin at this concentration and do not affect the acetylation status of histones. Second, Tubathians **2a–d** and control molecule Tubastatin A were tested at a range of concentrations (10, 50, 100, 500 and 1000 nM), revealing that these compounds already presented a maximal acetyl α-tubulin/α-tubulin ratio at a concentration of 100 nM. Finally, also the newly synthesized Tubathian analogs **3i–m** were tested at a lower concentration of 10 nM, pointing to the conclusion that compound **3k** (together with control substance Tubastatin A) demonstrated an even more pronounced activity than the other compounds (for more details, see ESI†).

With a strong HDAC inhibition profile for this Tubathian family in hand, the following step involved acquirement of *in vitro* 'ADME' (absorption, distribution, metabolism, and excretion) and 'Tox' (toxicity) data to know whether further optimization of these compounds in the framework of drug development is appropriate. Therefore, molecules **2a–d** as representative Tubathian 'mother structures' were preliminary screened for their capability to inhibit cytochrome P450 (cytochrome P450 inhibition can cause unanticipated adverse reactions or therapeutic failures), hERG safety (to exclude potential cardiotoxicity, as inhibition of the hERG might result in fatal ventricular tachyarrhythmia), microsomal stability in mouse and human (to measure *in vitro* intrinsic clearance), and plasma protein binding in mouse and human (the less bound a compound is to proteins in blood plasma, the more efficiently it can diffuse or traverse cell membranes) (Table 3). Apparently, whereas sulfides **2a** and **2b** were shown to inhibit the cytochrome P450 enzymes at low micromolar concentrations, which is harmful for possible drug–drug interactions *in vivo*, the sulfones **2c** and **2d** scored much better in this regard. The same can be stated for the hERG safety, showing sulfides **2a** and **2b** to be inferior as compared to sulfones **2c** and **2d**. In the microsomal stability assay and the plasma protein binding assay, sulfides **2a** and **2b** seemed difficult to detect, this in contrast to sulfones **2c** and **2d** which showed acceptable values in both assays. In summary, sulfones **2c** and **2d** clearly demonstrated a much better preliminary ADME/Tox profile than sulfides **2a** and **2b** and might thus be considered as potential lead compounds for further elaboration in future research. Additionally, a preliminary ADME/Tox screening of compounds **3i–m** concerning cytochrome P450 inhibition and microsomal stability was conducted (Table 4). From the cytochrome P450 inhibition data, it can be concluded that compounds **3j**, **3l** and **3m** display the best profile, with compound **3m** showing no P450 inhibition at all. The microsomal stability assays reveal that six-membered sulfoxides **3i** and **3j** and five-membered sulfones **3l** and **3m** have an improved stability over six-membered sulfones **2c**, **2d** and **3k**. In summary,

Table 3 Preliminary ADME/Tox screening of representative compounds **2a–d**

Compound	CYP1A2 (IC_{50} μM)	CYP2C9 (IC_{50} μM)	CYP2C19 (IC_{50} μM)	CYP2D6 (IC_{50} μM)	CYP3A4 (IC_{50} μM)	hERG (IC_{50} μM)
2a	>50	4.7	1.3	9.6	2.1	9.1
2b	>50	3.7	1.3	9.5	1.8	5.1
2c	>50	>50	19.9	>50	15	>11
2d	>50	11.8	>50	>50	9.7	>11

Compound	Mouse MS (μl min^{-1} mg^{-1})	Mouse MS $t_{1/2}$ (min)	Human MS (μl min^{-1} mg^{-1})	Human MS $t_{1/2}$ (min)	Mouse PPB (%)	Human PPB (%)
2a	<LOQ	<LOQ	<LOQ	<LOQ	<LOQ	<LOQ
2b	58.3	11.9	28.7	24.1	<LOQ	<LOQ
2c	16.2	42.7	26.5	26.1	69.8	62.7
2d	22.6	30.6	47.0	14.7	58.3	52.5

<LOQ: peak areas below limit of quantification.

Table 4 Preliminary ADME/Tox screening of compounds **3i–m**

Compound	CYP1A2 (IC_{50} μM)	CYP2C9 (IC_{50} μM)	CYP2C19 (IC_{50} μM)	CYP2D6 (IC_{50} μM)	CYP3A4 (IC_{50} μM)
3i	>50	36.9	15.4	39.8	8.5
3j	>50	>50	>50	>50	28.8
3k	>50	14.9	30.3	14.1	8.2
3l	>50	>50	16.3	>50	>50
3m	>50	>50	>50	>50	>50

Compound	Mouse MS (μl min^{-1} mg^{-1})	Mouse MS t1/2 (min)	Human MS (μl min^{-1} mg^{-1})	Human MS t1/2 (min)
3i	<2.1	>328	<2.3	>313
3j	8.8	79.1	<2.1	>340
3k	8.2	53.2	13.0	7.6
3l	7.8	89.0	<2.1	>335
3m	10.1	68.9	2.8	247.5

further investigation of six-membered sulfoxide **3j** and five-membered sulfones **3l** and **3m** seems appropriate from an ADME/Tox point of view.

In a final assay, the genotoxicity of six-membered sulfone **2c** and five-membered sulfone **3l** as representative examples was evaluated, bearing in mind the known potential mutagenicity associated with hydroxamic acids.[14,15] The Ames fluctuation test toward four strains of *Salmonella typhimurium* (TA98, TA100, TA1535 and TA1537), with and without metabolic activation by using rat liver S9 fraction, revealed that both compounds were only mutagenic toward strain TA1537, with and without S9, starting at a concentration of 50 μM (for more details, see ESI†). No mutagenicity was detected toward the other strains.

Conclusions

Thirteen novel Tubathian analogs were synthesized and, together with four previously developed analogs, evaluated in depth as HDAC6 inhibitors. The nine *para*-substituted compounds showed the best HDAC6 IC_{50}-values and proved to be selective inhibitors in cells. A detailed study of five selected representatives revealed that these Tubathian analogs preferentially inhibit HDAC6, although also a moderate affinity for class IIa HDACs (especially HDAC7 and 9) should be recognized. ADME/Tox evaluation demonstrated that sulfones **2c** and **2d** display a better preliminary ADME/Tox profile than the corresponding sulfides **2a** and **2b** and pointed to six-membered sulfoxide **3j** and five-membered sulfones **3l** and **3m** as promising chemical entities. Therefore, further research should be focused on these oxidized analogs as valuable lead structures in the pursuit of novel selective HDAC6 inhibitors.

Experimental section

Chemistry. General methods

^{1}H NMR, ^{13}C NMR and ^{19}F NMR spectra were recorded at 400, 100.6 or 376.5 MHz (Bruker Avance III) with $CDCl_3$ or [D_6] DMSO as the solvent and tetramethylsilane as the internal standard. Mass spectra were obtained with a mass spectrometer Agilent 1100, 70 eV. IR spectra were measured with a Spectrum One FT-IR spectrophotometer. High resolution electron spray (ES) mass spectra were obtained with an Agilent Technologies 6210 series time-of-flight instrument. Melting points of crystalline compounds were measured with a Kofler Bench, type WME Heizbank of Wagner & Munz. The purity of all tested compounds was assessed by ^{1}H NMR analysis and/or HPLC analysis, confirming a purity of ≥95%.

Representative procedure for the synthesis of sulfides 6a–f

To a solution of phenyl hydrazine hydrochloride **4a** (12 mmol) and 4,5-dihydro-3(2*H*)-thiophenone **5b** (12 mmol) in methanol (50 mL), was added $Bi(NO_3)_3{\cdot}5H_2O$ (2.4 mmol). After being stirred for 3.5 h under reflux, the reaction mixture was poured into water (100 mL), and bismuth nitrate was removed through filtration over celite. The crude product was extracted with ethyl acetate (100 mL), washed with saturated $NaHCO_3$ (100 mL), brine (100 mL) and dried over anhydrous $MgSO_4$. Filtration of the drying agent and removal of the solvent *in vacuo* afforded the crude cyclic thioether **6c**, which was purified by means of column chromatography (EtOAc/PE 1/5) to provide pure 2,3-dihydrothieno[3,2-*b*]indole **6c** (3.7 mmol, 31%). The synthesis of 1,2,4,9-tetrahydro-3-thia-9-azafluorene **6a** and 6-fluoro-1,2,4,9-tetrahydro-3-thia-9-azafluorene **6b** has already been described previously.[9] 7-Bromo-2,3-dihydrothieno[3,2-*b*]indole **6f** was not easily purified because it contained the corresponding sulfoxide as a side product and was therefore used as an intermediate for further transformation.

6-Bromo-1,2,4,9-tetrahydro-3-thia-9-azafluorene 6c. (reaction time 22 h) **^{1}H NMR** (400 MHz, $CDCl_3$): δ 3.00–3.02 (m, 4H), 3.80 (s, 2H), 7.16 (d, J = 8.5 Hz, 1H), 7.23 (d × d, J = 8.5, 1.9 Hz, 1H), 7.57 (d, J = 1.9 Hz, 1H), 7.83 (bs, 1H). **^{13}C NMR** (100.6 MHz, $CDCl_3$): δ 22.5, 25.2, 25.6, 106.7, 111.9, 112.8, 120.3, 124.4, 128.7, 133.1, 134.6. **MS** (70 eV): m/z (%) = 268/70 ($[M + 1]^+$, 58). **HRMS** (ESI) m/z for $C_{11}H_{11}BrNS$ $[M + H]^+$ calcd 269.9770, found 269.9769. Yellow powder. Recrystallisation from EtOH, yield 43%. Mp = 169.5 °C.

2,3-Dihydrothieno[3,2-*b*]indole 6d. ^{1}**H NMR** (400 MHz, $CDCl_3$): δ 3.20 and 3.83 (2 × t, J = 7.9 Hz, 2 × 2H), 7.07–7.15 (m, 2H), 7.28–7.31 (m, 1H), 7.36–7.38 (m, 1H), 7.97 (bs, 1H). ^{13}**C NMR** (100.6 MHz, $CDCl_3$): δ 28.4, 37.6, 111.6, 113.1, 118.7, 120.0, 121.4, 123.1, 137.1, 140.5. **MS** (70 eV): m/z (%) = 174 ([M − 1]$^-$, 100). **HRMS** (ESI) m/z for $C_{10}H_{10}NS$ [M + H]$^+$ calcd 176.0529, found 176.0526. Brown-orange powder. Column chromatography R_f (SiO_2) = 0.23, EtOAc/PE (1/5), yield 31%. Mp = 144.0 °C.

7-Fluoro-2,3-dihydrothieno[3,2-*b*]indole 6e. ^{1}**H NMR** (400 MHz, $CDCl_3$): δ 3.18 and 3.81 (2 × t, J = 7.9 Hz, 2 × 2H), 6.86 (t × d, J = 9.0, 2.5 Hz, 1H), 7.02 (d × d, J = 9.4, 2.5 Hz, 1H), 7.18 (d × d, J = 9.0, 4.3 Hz, 1H), 7.95 (bs, 1H). ^{13}**C NMR** (100.6 MHz, $CDCl_3$): δ 28.4, 37.6, 103.8 (d, J = 24.3 Hz), 109.5 (d, J = 26.3 Hz), 112.1 (d, J = 9.7 Hz), 113.2 (d, J = 4.4 Hz), 123.2 (d, J = 10.5 Hz), 136.9, 139.3, 157.9 (d, J = 234.9 Hz). ^{19}**F NMR** (376.5 MHz, $CDCl_3$): δ (−123.90)–(−123.84) (m). **MS** (70 eV): m/z (%) = 192 ([M − 1]$^-$, 100). **HRMS** (ESI) m/z for $C_{10}H_7FNS$ [M − H]$^-$, calcd 192.0289, found 192.0291. Brown-orange powder. Column chromatography R_f (SiO_2) = 0.20, EtOAc/PE (1/4), yield 30%. Mp = 133.5 °C.

Representative procedure for the synthesis of sulfoxides 7a–c

To a solution of 1,2,4,9-tetrahydro-3-thia-9-azafluorene **6a** (5 mmol) in tetrahydrofuran (50 mL) was added boron trifluoride diethyl etherate (20 mmol) at −20 °C under nitrogen atmosphere. Then *m*-chloroperbenzoic acid was added (5 mmol) at −20 °C and the mixture was stirred at −20 °C for 2 h. After two hours the reaction mixture was poured into a saturated solution of $NaHCO_3$ (100 mL) and subsequently extracted with ethyl acetate (100 mL). The organic phase was washed with water (2 × 50 mL), brine (50 mL) and dried over anhydrous $MgSO_4$. Filtration of the drying agent and removal of the solvent *in vacuo* afforded the crude cyclic sulfoxide **7a**, which was purified by recrystallization from EtOH to provide pure 1,2,4,9-tetrahydro-3-thia-9-azafluorene-3-oxide **7a** (4.15 mmol, 83%).

1,2,4,9-Tetrahydro-3-thia-9-azafluorene-3-oxide 7a. ^{1}**H NMR** (400 MHz, d_6-DMSO): δ 3.03–3.34 (m, 4H), 3.93 and 4.21 (2 × d, J = 15.1 Hz, 2 × 1H), 6.98 (t, J = 7.5 Hz, 1H), 7.06 (t, J = 7.5 Hz, 1H), 7.30 (d, J = 7.5 Hz, 1H), 7.42 (d, J = 7.5 Hz, 1H), 11.10 (bs, 1H). ^{13}**C NMR** (100.6 MHz, d_6-DMSO): δ 17.7, 44.5, 45.1, 98.9, 111.3, 117.7, 119.1, 121.5, 127.8, 132.3, 136.1. **MS** (70 eV): m/z (%) = 206 ([M + 1]$^+$, 90). **HRMS** (ESI) m/z for $C_{11}H_{12}NOS$ [M + H]$^+$ calcd 206.0634, found 206.0638. Beige powder. Recrystallization from EtOH, yield 83%. Mp > 260.0 °C.

6-Fluoro-1,2,4,9-tetrahydro-3-thia-9-azafluorene-3-oxide 7b. ^{1}**H NMR** (400 MHz, d_6-DMSO): δ 3.02–3.33 (m, 4H), 3.93 and 4.16 (2 × d, J = 15.2 Hz, 2 × 1H), 6.89 (t × d, J = 9.0, 2.6 Hz, 1H), 7.22 (d × d, J = 9.9, 2.6 Hz, 1H), 7.29 (d × d, J = 9.0, 4.5 Hz, 1H), 11.14 (bs, 1H). ^{13}**C NMR** (100.6 MHz, d_6-DMSO): δ 17.5, 44.2, 44.8, 99.4 (d, J = 4.4 Hz), 102.8 (d, J = 23.6 Hz), 109.3 (d, J = 25.9 Hz), 112.2 (d, J = 9.7 Hz), 128.2 (d, J = 10.0 Hz), 132.7, 134.5, 157.3 (d, J = 231.4 Hz). ^{19}**F NMR** (376.5 MHz, d_6-DMSO): δ (−125.11)–(−125.05) (m). **MS** (70 eV): m/z (%) = 224 ([M + 1]$^+$, 100). **HRMS** (ESI) m/z for $C_{11}H_{11}FNOS$ [M + H]$^+$ calcd 224.0540, found 224.0548. Yellow powder. Recrystallization from EtOH, yield 68%. Mp = 242.0 °C.

7-Bromo-2,3-dihydrothieno[3,2-*b*]indole-1-oxide 7c. ^{1}**H NMR** (400 MHz, d_6-DMSO): δ 3.15–3.22, 3.28–3.33, 3.59–3.67 and 3.96–4.03 (4 × m, 4 × 1H), 7.33 (d × d, J = 8.6, 1.9 Hz, 1H), 7.43 (d, J = 8.6 Hz, 1H), 7.83 (d, J = 1.9 Hz, 1H), 12.07 (bs, 1H). ^{13}**C NMR** (100.6 MHz, d_6-DMSO): δ 24.0, 59.0, 113.9, 115.0, 120.8, 120.9, 124.5, 125.3, 140.1, 153.4. **MS** (70 eV): m/z (%) 270/2 ([M + 1]$^+$, 100). **HRMS** (ESI) m/z for $C_{10}H_9BrNOS$ [M + H]$^+$ calcd 269.9583, found 269.9593. Black powder. Recrystallization from EtOH, yield 41%. Mp = 191.0 °C.

Representative procedure for the synthesis of sulfones 8a–e

To a solution of 6-bromo-1,2,4,9-tetrahydro-3-thia-9-azafluorene **6c** (5 mmol) in tetrahydrofuran (50 mL) was added *m*-chloroperbenzoic acid in tetrahydrofuran (15 mmol) at 0 °C. The mixture was stirred at room temperature for 2 h. The solvent was removed *in vacuo* and the residue was dissolved in ethyl acetate (100 mL). The solution was washed with saturated aqueous sodium sulfite (30 mL), water (30 mL), brine (2 × 30 mL), and dried over anhydrous $MgSO_4$. Filtration of the drying agent and removal of the solvent *in vacuo* afforded the crude cyclic sulfone **8c**, which was purified by recrystallization from EtOH to provide pure 6-bromo-1,2,4,9-tetrahydro-3-thia-9-azafluorene-3,3-dioxide **8c** (3.05 mmol, 61%). The synthesis of 1,2,4,9-tetrahydro-3-thia-9-azafluorene-3,3-dioxide **8a** and 6-fluoro-1,2,4,9-tetrahydro-3-thia-9-azafluorene-3,3-dioxide **8b** has been described previously.[9]

6-Bromo-1,2,4,9-tetrahydro-3-thia-9-azafluorene-3,3-dioxide 8c. ^{1}**H NMR** (400 MHz, d_6-DMSO): δ 3.27 and 3.48 (2 × t, J = 6.1 Hz, 2 × 2H), 4.44 (s, 2H), 7.20 (d × d, J = 8.6, 1.5 Hz, 1H), 7.30 (d, J = 8.6 Hz, 1H), 7.65 (d, J = 1.5 Hz, 1H), 11.36 (bs, 1H). ^{13}**C NMR** (100.6 MHz, d_6-DMSO): δ 23.1, 47.1, 48.6, 101.9, 111.9, 113.4, 120.3, 124.3, 129.1, 132.4, 135.2. **MS** (70 eV): m/z (%) 322/4 (M^+ + 23, 55). **HRMS** (ESI) m/z for $C_{11}H_{10}BrNO_2S$ [M − H]$^-$ calcd 297.9543, found 297.9541. Brown powder. Recrystallization from EtOH, yield 61%. Mp = 215.0 °C.

2,3-Dihydrothieno[3,2-*b*]indole-1,1-dioxide 8d. ^{1}**H NMR** (400 MHz, d_6-DMSO): δ 3.44 and 3.90 (2 × t, J = 6.6 Hz, 2 × 2H), 7.17–7.21 (m, 1H), 7.24–7.28 (m, 1H), 7.48–7.50 (m, 1H), 7.54–7.56 (m, 1H), 12.00 (bs, 1H). ^{13}**C NMR** (100.6 MHz, d_6-DMSO): δ 21.4, 57.6, 113.3, 116.1, 118.4, 119.4, 121.9, 123.7, 140.8, 147.7. **MS** (70 eV): m/z (%) = 208 ([M + 1]$^+$, 30), 225 [M + NH_4^+], 100). **HRMS** (ESI) m/z for $C_{10}H_{10}NO_2S$ [M + H]$^+$ calcd 208.0427, found 208.0429. Beige powder. Recrystallization from EtOH, yield 52%. Mp = 260.0 °C.

7-Fluoro-2,3-dihydrothieno[3,2-*b*]indole-1,1-dioxide 8e. ^{1}**H NMR** (400 MHz, d_6-DMSO): δ 3.44 and 3.89 (2 × t, J = 6.6 Hz, 2 × 2H), 7.12 (t × d, J = 9.1, 2.5 Hz, 1H), 7.33 (d × d, J = 9.3, 2.5 Hz, 1H), 7.51 (d × d, J = 9.1, 4.5 Hz, 1H), 12.10 (bs, 1H). ^{13}**C NMR** (100.6 MHz, d_6-DMSO): δ 21.5, 57.6, 103.8 (d, J = 25.1 Hz), 111.7 (d, J = 25.7 Hz), 114.6 (d, J = 9.8 Hz), 116.2 (d, J = 4.4 Hz, $C_{quat,arom}$), 119.6 (d, J = 11.3 Hz), 137.4, 149.3, 158.3 (d, J = 235.3 Hz). ^{19}**F NMR** (376.5 MHz, d_6-DMSO): δ (−121.35)–(−121.29) (m). **MS** (70 eV): m/z (%) = 243 ([M + NH_4^+], 100). **HRMS** (ESI) m/z for $C_{10}H_9FNO_2S$ [M + H]$^+$ calcd 226.0333,

found 226.0334. Pink powder. Recrystallization from EtOH, yield 70%. Mp > 260.0 °C.

Representative procedure for the synthesis of 6-phenyl-1,2,4,9-tetrahydro-3-thia-9-azafluorene-3,3-dioxide 8f

6-Bromo-1,2,4,9-tetrahydro-3-thia-9-azafluorene-3,3-dioxide **8c** (2 mmol) was dissolved in toluene (15 mL), and to this solution an aqueous solution of sodium carbonate (7 mL, 2 M) and a solution of phenylboronic acid (4 mmol) in ethanol (7 mL) were added. This mixture was then flushed with nitrogen gas for 10 minutes before tetrakis(triphenylphosphine)-palladium(0) (0.08 mmol) was added, and the reaction mixture was heated under reflux for 8 hour. The reaction mixture was then poured into brine (20 mL) and extracted with EtOAc (3 × 20 mL). The combined organic fraction was washed with brine (3 × 15 mL), dried ($MgSO_4$), filtered and evaporated under vacuum. Purification through recrystallization from EtOH yielded 6-phenyl-1,2,4,9-tetrahydro-3-thia-9-azafluorene-3,3-dioxide **8f** (1.2 mmol, 60%) as a light brown powder.

6-Phenyl-1,2,4,9-tetrahydro-3-thia-9-azafluorene-3,3-dioxide 8f. **^{1}H NMR** (400 MHz, d_6-DMSO): δ 3.29 and 3.50 (2 × t, J = 6.2 Hz, 2 × 2H), 4.51 (s, 2H), 7.30 (t, J = 7.4 Hz, 1H), 7.39–7.43 (m, 2H), 7.45 (t, J = 7.4 Hz, 2H), 7.68 (d, J = 7.4 Hz, 2H), 7.74 (s, 1H), 11.21 (bs, 1H). **^{13}C NMR** (100.6 MHz, d_6-DMSO): δ 23.2, 47.2, 48.9, 102.5, 111.8, 116.1, 121.2, 126.8, 127.1, 127.9, 129.2, 131.4, 131.9, 136.2, 142.1. **MS** (70 eV): m/z (%) 298 ([M + 1]$^+$, 40). **HRMS** (ESI) m/z for $C_{17}H_{16}NO_2S$ [M + H]$^+$ calcd 298.0896, found 298.0902. Light brown powder. Recrystallization from EtOH, yield 60%. Mp = 237.0 °C.

Representative procedure for the synthesis of *N*-methoxycarbonylbenzyl-1,2,4,9-tetrahydro-3-thia-9-azafluorenes 10a–m

1,2,4,9-Tetrahydro-3-thia-9-azafluorene **6a** (6 mmol) and sodium hydride (60 wt% in mineral oil, 6 mmol) were placed under nitrogen and dissolved in DMF (10 mL). After stirring for 30 minutes, methyl 3-(bromomethyl)benzoate **9** (6 mmol) and potassium iodide (0.06 mmol) were added. The mixture was heated to 80 °C for 2 h, after which it was quenched with water (30 mL), followed by addition of ethyl acetate (30 mL). The aqueous layer was extracted with ethyl acetate (2 × 10 mL) and the combined organic layers were washed with water (2 × 20 mL) and brine (15 mL), dried ($MgSO_4$) and concentrated *in vacuo*. Purification by means of column chromatography (EtOAc/PE 1/10, R_f = 0.18) afforded pure *N*-(3-methoxycarbonylbenzyl)-1,2,4,9-tetrahydro-3-thia-9-azafluorene **10a** (2.46 mmol, 41%).

***N*-(3-Methoxycarbonylbenzyl)-1,2,4,9-tetrahydro-3-thia-9-azafluorene 10a.** **^{1}H NMR** (400 MHz, $CDCl_3$): δ 2.92 and 3.04 (2 × t, J = 5.8 Hz, 2 × 2H), 3.93 (s, 3H), 3.95 (s, 2H), 5.33 (s, 2H), 7.03–7.05 (m, 1H), 7.13–7.20 (m, 2H), 7.24–7.26 (m, 1H), 7.33 (t, J = 7.7 Hz, 1H), 7.52–7.55 (m, 1H), 7.90–7.95 (m, 2H). **^{13}C NMR** (100.6 MHz, $CDCl_3$): δ 23.1, 24.1, 25.9, 46.0, 52.3, 107.3, 108.9, 117.7, 119.5, 121.7, 126.8, 127.4, 128.7, 129.1, 130.5, 130.6, 134.5, 135.7, 138.2, 166.8. **MS** (70 eV): m/z (%) = 338 ([M + 1]$^+$, 90). **HRMS** (ESI) m/z for $C_{20}H_{20}NO_2S$ [M + H]$^+$ calcd 338.1209, found 338.1219. White-yellow powder. Column chromatography R_f (SiO_2) = 0.18, EtOAc/PE (1/10), yield 41%. Mp = 115.0 °C.

***N*-(3-Methoxycarbonylbenzyl)-6-fluoro-1,2,4,9-tetrahydro-3-thia-9-azafluorene 10b.** **^{1}H NMR** (400 MHz, $CDCl_3$): δ 2.89 and 3.00 (2 × t, J = 5.7 Hz, 2 × 2H), 3.85 (s, 2H), 3.90 (s, 3H), 5.27 (s, 2H), 6.87 (t × d, J = 9.1, 2.5 Hz, 1H), 6.99–7.01 (m, 1H), 7.08–7.15 (m, 2H), 7.32 (t, J = 7.7 Hz, 1H), 7.84 (s, 1H), 7.90–7.93 (m, 1H). **^{13}C NMR** (100.6 MHz, $CDCl_3$): δ 22.9, 24.2, 25.8, 46.2, 52.3, 103.0 (d, J = 23.6 Hz), 107.4 (d, J = 4.4 Hz), 109.5 (d, J = 9.6 Hz), 109.7 (d, J = 26.0 Hz), 127.1 (d, J = 9.7 Hz), 127.3, 128.8, 129.2, 130.4, 130.8, 132.2, 136.3, 137.9, 157.9 (d, J = 235.0 Hz), 166.7. **^{19}F NMR** (376.5 MHz, $CDCl_3$): δ (−134.64)–(−124.52) (m). **MS** (70 eV): m/z (%) = 356 ([M + 1]$^+$, 100). **HRMS** (ESI) m/z for $C_{20}H_{19}FNO_2S$ [M + H]$^+$ calcd 356.1115, found 356.1131. White-yellow powder. Column chromatography R_f (SiO_2) = 0.16, EtOAc/PE (1/10), yield 50%. Mp = 97.0 °C.

***N*-(3-Methoxycarbonylbenzyl)-1,2,4,9-tetrahydro-3-thia-9-azafluorene-3,3-dioxide 10c.** **^{1}H NMR** (400 MHz, d_6-DMSO): δ 3.21 and 3.51 (2 × t, J = 6.2 Hz, 2 × 2H), 3.82 (s, 3H), 4.51 (s, 2H), 5.53 (s, 2H), 7.06–7.10 (m, 1H), 7.14–7.18 (m, 1H), 7.22–7.25 (m, 1H), 7.45–7.52 (m, 3H), 7.78 (s, 1H), 7.85 (d, J = 7.9 Hz, 1H). **^{13}C NMR** (100.6 MHz, d_6-DMSO): δ 22.4, 45.9, 46.7, 48.4, 52.7, 102.8, 110.3, 118.3, 120.0, 122.5, 126.6, 127.7, 128.6, 129.8, 130.5, 131.5, 131.6, 137.1, 139.3, 166.4. **MS** (70 eV): m/z (%) = 370 ([M + 1]$^+$, 7), 387 ([M + NH_4^+], 100). **HRMS** (ESI) m/z for $C_{20}H_{20}NO_4S$ [M + H]$^+$, calcd 370.1108, found 370.1111. Yellow powder. Column chromatography R_f (SiO_2) = 0.26, EtOAc/PE (4/5), yield 21%. Mp = 200.0 °C.

***N*-(3-Methoxycarbonylbenzyl)-6-fluoro-1,2,4,9-tetrahydro-3-thia-9-azafluorene-3,3-dioxide 10d.** **^{1}H NMR** (400 MHz, d_6-DMSO): δ 3.21 and 3.50 (2 × t, J = 6.1 Hz, 2 × 2H), 3.83 (s, 3H), 4.48 (s, 2H), 5.54 (s, 2H), 7.01 (t × d, J = 9.2, 2.5 Hz, 1H), 7.22 (d, J = 7.9 Hz, 1H), 7.33 (d × d, J = 9.3, 2.5 Hz, 1H), 7.47 (t, J = 7,9 Hz, 1H), 7.51 (d × d, J = 9.2, 4.3 Hz, 1H), 7.77 (s, 1H), 7.86 (d, J = 7.9 Hz, 1H). **^{13}C NMR** (100.6 MHz, d_6-DMSO): δ 22.5, 46.1, 46.6, 48.3, 52.7, 103.1 (d, J = 4.6 Hz), 103.5 (d, J = 24.0 Hz), 110.4 (d, J = 25.9 Hz), 111.5 (d, J = 9.6 Hz), 126.9 (d, J = 10.3 Hz), 127.7, 128.7, 129.8, 130.5, 131.6, 133.5, 133.8, 139.1, 157.7 (d, J = 233.0 Hz), 166.4. **^{19}F NMR** (376.5 MHz, d_6-DMSO): δ (−124.05)–(−123.99) (m). **MS** (70 eV): m/z (%) = 405 ([M + NH_4^+], 100). **HRMS** (ESI) m/z for $C_{20}H_{19}FNO_4S$ [M + H]$^+$ calcd 388.1013, found 388.1019. Beige powder. Recrystallization from EtOH, yield 67%. Mp = 214.0 °C.

***N*-(3-Methoxycarbonylbenzyl)-6-phenyl-1,2,4,9-tetrahydro-3-thia-9-azafluorene-3,3-dioxide 10e.** **^{1}H NMR** (400 MHz, d_6-DMSO): δ 3.24 and 3.52 (2 × t, J = 5.9 Hz, 2 × 2H), 3.83 (s, 3H), 4.57 (s, 2H), 5.57 (s, 2H), 7.26 (d, J = 7.7 Hz, 1H), 7.32 (t, J = 7.3 Hz, 1H), 7.44–7.50 (m, 4H), 7.58 (d, J = 8.6 Hz, 1H), 7.70 (d, J = 7.3 Hz, 2H), 7.81–7.83 (m, 2H), 7.87 (d, J = 7.7 Hz, 1H). **^{13}C NMR** (100.6 MHz, d_6-DMSO): δ 22.5, 46.1, 46.7, 48.5, 52.7, 103.4, 110.7, 116.6, 121.7, 126.9, 127.2, 127.7, 128.6, 129.3, 129.8, 130.5, 131.6, 132.3, 132.6, 136.7, 139.3, 141.8, 166.4. **MS** (70 eV): m/z (%) 446 ([M + 1]$^+$, 80). **HRMS** (ESI) m/z for $C_{26}H_{27}N_2O_4S$ [M + NH_4]$^+$ calcd 463.1686, found 463.1694. Light brown powder. Recrystallization from EtOH, yield 60%. Mp = 201.0 °C.

***N*-(3-Methoxycarbonylbenzyl)-2,3-dihydrothieno[3,2-*b*]indole-1,1-dioxide 10f.** **^{1}H-NMR** (400 MHz, d_6-DMSO): δ 3.44 (t, J = 6.5 Hz, 2H), 3.84 (s, 3H), 3.95 (t, J = 6.5 Hz, 2H), 5.57 (s, 2H), 7.23–7.32 (m, 2H), 7.42–7.45 (m, 1H), 7.49–7.53 (m, 1H), 7.59–7.62 (m, 2H), 7.88–7.91 (m, 2H). **^{13}C-NMR** (100.6 MHz, d_6-DMSO): δ 21.0, 46.9, 52.7, 57.4, 112.3, 116.2, 118.8, 119.3, 122.5, 124.0, 128.2, 129.0, 129.9, 130.6, 132.3, 137.9, 141.0, 148.5, 166.4. **MS** (70 eV): m/z (%) = 373 ([M + NH_4^+], 100). **HRMS** (ESI) m/z for $C_{19}H_{18}NO_4S$ $[M + H]^+$ calcd 356.0951, found 356.0958. White powder. Recrystallization from EtOH, yield 72%. Mp = 210.5 °C.

***N*-(3-Methoxycarbonylbenzyl)-7-fluoro-2,3-dihydrothieno[3,2-*b*]indole-1,1-dioxide 10g.** **^{1}H NMR** (400 MHz, d_6-DMSO): δ 3.44 (t, J = 6.5 Hz, 2H), 3.84 (s, 3H), 3.95 (t, J = 6.5 Hz, 2H), 5.57 (s, 2H), 7.18 (t × d, J = 9.2, 2.5 Hz, 1H), 7.39–7.44 (m, 2H), 7.49–7.53 (m, 1H), 7.63 (d × d, J = 9.2, 4.3 Hz, 1H), 7.89–7.91 (m, 2H). **^{13}C NMR** (100.6 MHz, d_6-DMSO): δ 21.1, 47.1, 52.7, 57.3, 104.3 (d, J = 25.2 Hz), 112.1 (d, J = 26.0 Hz), 113.7 (d, J = 9.9 Hz), 116.2 (d, J = 4.4 Hz), 119.5 (d, J = 11.2 Hz), 128.2, 129.1, 130.0, 130.6, 132.3, 137.6, 137.7, 150.1, 158.7 (d, J = 236.9 Hz), 166.4. **^{19}F NMR** (376.5 MHz, d_6-DMSO): δ (−120.57)–(−120.50) (m). **MS** (70 eV): m/z (%) = 391 ([M + NH_4^+], 100). **HRMS** (ESI) m/z for $C_{19}H_{17}FNO_4S$ $[M + H]^+$ calcd 374.0857, found 374.0857. White powder. Recrystallization from EtOH, yield 60%. Mp = 222.0 °C.

***N*-(3-Methoxycarbonylbenzyl)-7-bromo-2,3-dihydrothieno[3,2-*b*]indole-1-oxide 10h.** **^{1}H NMR** (400 MHz, $CDCl_3$): δ 3.01–3.07 (m, 1H), 3.45–3.51 (m, 1H), 3.61–3.69 (m, 1H), 3.91–4.00 (m, 1H), 3.91 (s, 3H), 5.29 and 5.35 (2 × d, J = 16.4 Hz, 2 × 1H), 7.13 (d, J = 8.8 Hz, 1H), 7.19 (d, J = 7.7 Hz, 1H), 7.34 (d × d, J = 8.8, 1.8 Hz, 1H), 7.40 (t, J = 7.7 Hz, 1H), 7.90 (s, 1H), 7.96 (d, J = 1.8 Hz, 1H), 7.99 (d, J = 7.7 Hz, 1H). **^{13}C NMR** (100.6 MHz, $CDCl_3$): δ 23.8, 48.9, 52.4, 58.3, 112.0, 115.5, 120.9, 122.1, 124.3, 126.3, 127.8, 129.5, 129.6, 130.9, 131.2, 135.8, 140.1, 152.4, 166.4. **MS** (70 eV): m/z (%) 418/20 ([M + 1]$^+$, 100). **HRMS** (ESI) m/z for $C_{19}H_{17}BrNO_3S$ $[M + H]^+$ calcd 418.0107, found 418.0125. Brown powder. Column chromatography R_f (SiO_2) = 0.23, acetone/PE (1/1), yield 54%. Mp = 187.5 °C.

***N*-(4-Methoxycarbonylbenzyl)-1,2,4,9-tetrahydro-3-thia-9-azafluorene-3-oxide 10i.** **^{1}H NMR** (400 MHz, d_6-DMSO): δ 2.98–3.16 (m, 3H), 3.28–3.38 (m, 1H), 3.82 (s, 3H), 4.03 and 4.23 (2 × d, J = 15.4 Hz, 2 × 1H), 5.53 (s, 2H), 7.05–7.14 (m, 2H), 7.17 (d, J = 8.3 Hz, 2H), 7.43 (d, J = 8.0 Hz, 1H), 7.52 (d, J = 7.5 Hz, 1H), 7.90 (d, J = 8.3 Hz, 2H). **^{13}C NMR** (100.6 MHz, d_6-DMSO): δ 16.6, 44.0, 44.8, 45.9, 52.6, 99.8, 110.1, 118.1, 119.8, 122.0, 127.1, 127.6, 129.1, 130.1, 133.2, 136.7, 144.2, 166.4. **MS** (70 eV): m/z (%) = 354 ([M + 1]$^+$, 70). **HRMS** (ESI) m/z for $C_{20}H_{20}NO_3S$ $[M + H]^+$ calcd 354.1158, found 354.1153. Brown powder. Recrystallization from EtOH, yield 47%. Mp = 78.0 °C.

***N*-(4-Methoxycarbonylbenzyl)-6-fluoro-1,2,4,9-tetrahydro-3-thia-9-azafluorene-3-oxide 10j.** **^{1}H NMR** (400 MHz, d_6-DMSO): δ 2.97–3.14 (3H, m), 3.32–3.36 (m, 1H), 3.82 (s, 3H), 4.02 and 4.18 (2 × d, J = 15.3 Hz, 2 × 1H), 5.53 (s, 2H), 6.96 (t × d, J = 9.0, 2.5 Hz, 1H), 7.16 (d, J = 8.3 Hz, 2H), 7.33 (d × d, J = 9.7, 2.5 Hz, 1H), 7.45 (d × d, J = 9.0, 4.3 Hz, 1H), 7.90 (d, J = 8.3 Hz, 2H). **^{13}C NMR** (100.6 MHz, d_6-DMSO): δ 16.5, 43.7, 44.6, 46.1, 52.6, 100.1 (d, J = 4.4 Hz), 103.3 (d, J = 23.8 Hz), 109.8 (d, J = 26.0 Hz), 111.2 (d, J = 9.6 Hz), 127.1, 128.0 (d, J = 10.2 Hz), 129.1, 130.1, 133.4, 135.3, 143.9, 157.7 (d, J = 232.6 Hz), 166.4. **^{19}F NMR** (376.5 MHz, d_6-DMSO): δ (−124.41)–(−124.34) (m). **MS** (70 eV): m/z (%) = 372 ([M + 1]$^+$, 77). **HRMS** (ESI) m/z for $C_{20}H_{19}FNO_3S$ $[M + H]^+$ calcd 372.1064, found 372.1065. Brown powder. Recrystallization from EtOH, yield 42%. Mp = 135.5 °C.

***N*-(4-Methoxycarbonylbenzyl)-6-bromo-1,2,4,9-tetrahydro-3-thia-9-azafluorene-3,3-dioxide 10k.** **^{1}H NMR** (400 MHz, $CDCl_3$): δ 3.25–3.28 and 3.30–3.33 (2 × m, 2 × 2H), 3.90 (s, 3H), 4.37 (s, 2H), 5.32 (s, 2H), 7.01 (d, J = 8.5 Hz, 2H), 7.09 (d, J = 8.7 Hz, 1H), 7.30 (d × d, J = 8.7, 1.8 Hz, 1H), 7.57 (d, J = 1.8 Hz, 1H), 7.97 (d, J = 8.5 Hz, 2H). **^{13}C NMR** (100.6 MHz, $CDCl_3$): δ 22.2, 46.7, 47.2, 48.7, 52.3, 102.2, 111.0, 113.8, 120.4, 125.8, 125.9, 128.0, 130.0, 130.5, 131.4, 135.9, 141.3, 166.4. **MS** (70 eV): m/z (%) 448/50 ([M + 1]$^+$, 70). **HRMS** (ESI) m/z for $C_{20}H_{22}BrN_2O_4S$ [M + NH_4]$^+$ calcd 465.0478, found 465.0473. Light brown powder. Column chromatography R_f (SiO_2) = 0.25, EtOAc/PE (1/1), yield 80%. Mp = 191.0 °C.

***N*-(4-Methoxycarbonylbenzyl)-2,3-dihydrothieno[3,2-*b*]indole-1,1-dioxide 10l.** **^{1}H NMR** (400 MHz, d_6-DMSO): δ 3.44 (t, J = 6.5 Hz, 2H), 3.83 (s, 3H), 3.95 (t, J = 6.5 Hz, 2H), 5.57 (s, 2H), 7.23–7.31 (m, 2H), 7.35 (d, J = 8.4 Hz, 2H), 7.55–7.62 (m, 2H), 7.94 (d, J = 8.4 Hz, 2H). **^{13}C NMR** (100.6 MHz, d_6-DMSO): δ 20.9, 47.0, 52.6, 57.4, 112.2, 116.3, 118.8, 119.3, 122.5, 124.0, 127.8, 129.5, 130.2, 141.0, 142.5, 148.6, 166.3. **MS** (70 eV): m/z (%) = 356 ([M + 1]$^+$, 41), 373 ([M + NH_4^+], 100). **HRMS** (ESI) m/z for $C_{19}H_{18}NO_4S$ $[M + H]^+$ calcd 356.0951, found 356.0954. White powder. Recrystallization from EtOH, yield 60%. Mp = 226.5 °C.

***N*-(4-Methoxycarbonylbenzyl)-7-fluoro-2,3-dihydrothieno[3,2-*b*]indole-1,1-dioxide 10m.** **^{1}H NMR** (400 MHz, d_6-DMSO): δ 3.44 (t, J = 6.5 Hz, 2H), 3.84 (s, 3H), 3.95 (t, J = 6.5 Hz, 2H), 5.57 (s, 2H), 7.16 (t × d, J = 9.2, 2.5 Hz, 1H), 7.34 (d, J = 8.3 Hz, 2H), 7.41 (d × d, J = 9.1, 2.5 Hz, 1H), 7.59 (d × d, J = 9.2, 4.3 Hz, 1H), 7.94 (d, J = 8.3 Hz, 2H). **^{13}C NMR** (100.6 MHz, d_6-DMSO): δ 21.0, 47.2, 52.7, 57.3, 104.3 (d, J = 25.1 Hz), 112.1 (d, J = 25.8 Hz), 113.7 (d, J = 9.9 Hz), 116.3 (d, J = 4.5 Hz), 119.5 (d, J = 11.3 Hz), 127.8, 129.6, 130.2, 137.6, 142.2, 150.1, 158.7 (d, J = 236.9 Hz), 166.3. **^{19}F NMR** (376.5 MHz, d_6-DMSO): δ (−120.57)–(−120.51) (m). **MS** (70 eV): m/z (%) = 391 ([M + NH_4^+], 100). **HRMS** (ESI) m/z for $C_{19}H_{17}FNO_4S$ $[M + H]^+$ calcd 374.0857, found 374.0852. White powder. Recrystallization from EtOH, yield 80%. Mp = 243.0 °C.

Representative procedure for the synthesis of hydroxamic acids 3a–m

N-(3-Methoxycarbonylbenzyl)-1,2,4,9-tetrahydro-3-thia-9-azafluorene **10a** (1 mmol) was dissolved in THF (10 mL), and to this solution was added hydroxylamine (100 mmol) and subsequently potassium hydroxide in methanol (4 M, 50 mmol). The resulting mixture was stirred for an additional 10 minutes at room temperature, before it was poured into a saturated aqueous solution of $NaHCO_3$ (10 mL). This aqueous solution

was extracted two times with ethyl acetate, after which the combined organic fractions were washed with water (10 mL) and a saturated brine solution (10 mL), dried ($MgSO_4$), filtered and evaporated. Purification through recrystallization from EtOH yielded *N*-(3-hydroxycarbamoylbenzyl)-1,2,4,9-tetrahydro-3-thia-9-azafluorene **3a** (0.57 mmol, 57%) as a white-yellow powder. Note: the mixture was stirred at reflux temperature for the synthesis of hydroxamic acids **3d**, **3g** and **3m**.

***N*-(3-Hydroxycarbamoylbenzyl)-1,2,4,9-tetrahydro-3-thia-9-azafluorene 3a.** ^{1}**H NMR** (400 MHz, d_6-DMSO): δ 2.90 and 3.00 (2 × t, J = 5.5 Hz, 2 × 2H), 3.84 (s, 2H), 5.42 (s, 2H), 7.01–7.05 (m, 1H), 7.07–7.11 (m, 2H), 7.36 (t, J = 7.7 Hz, 1H), 7.42 (d, J = 7.7 Hz, 1H), 7.48 (d, J = 7.3 Hz, 1H), 7.54 (s, 1H), 7.58 (d, J = 7.7, 1H), 9.00 (bs, 1H), 11.19 (bs, 1H). ^{13}**C NMR** (100.6 MHz, d_6-DMSO): δ 22.7, 24.0, 25.6, 45.7, 106.8, 109.9, 118.0, 119.4, 121.5, 125.8, 125.9, 126.7, 129.2, 129.5, 133.7, 135.4, 135.7, 139.3, 164.6. **MS** (70 eV): m/z (%) = 339 ([M + 1]$^+$, 100). **HRMS** (ESI) m/z for $C_{19}H_{19}N_2O_2S$ [M + H]$^+$ calcd 339.1162, found 339.1159. White-yellow powder. Crystallization from EtOH, yield 57%. Mp = 124.5 °C.

***N*-(3-Hydroxycarbamoylbenzyl)-6-fluoro-1,2,4,9-tetrahydro-3-thia-9-azafluorene 3b.** ^{1}**H NMR** (400 MHz, d_6-DMSO): δ 2.89 and 2.99 (2 × t, J = 5.4 Hz, 2 × 2H), 3.81 (s, 2H), 5.42 (s, 2H), 6.92 (t × d, J = 9.1, 2.5 Hz, 1H), 7.07 (d, J = 7.7 Hz, 1H), 7.26 (d × d, J = 9.7, 2.5 Hz, 1H), 7.36 (t, J = 7.7 Hz, 1H), 7.44 (d × d, J = 9.1, 4.4 Hz, 1H), 7.51 (s, 1H), 7.59 (d, J = 7.7 Hz, 1H), 9.04 (bs, 1H), 11.14 (bs, 1H). ^{13}**C NMR** (100.6 MHz, d_6-DMSO): δ 22.6, 24.2, 25.5, 45.9, 103.1 (d, J = 23.4 Hz), 107.1 (d, J = 4.4 Hz), 109.3 (d, J = 25.8 Hz), 110.9 (d, J = 9.8 Hz), 125.7, 125.9, 127.0 (d, J = 10.1 Hz), 129.2, 129.4, 132.4, 133.7, 137.5, 139.0, 157.5 (d, J = 232.0 Hz), 164.5. ^{19}**F NMR** (376.5 MHz, d_6-DMSO): δ (−124.92)–(−124.86) (m). **MS** (70 eV): m/z (%) = 357 ([M + 1]$^+$, 100). **HRMS** (ESI) m/z for $C_{19}H_{18}FN_2O_2S$ [M + H]$^+$ calcd 357.1068, found 357.1062. Yellow powder. Crystallization from diethyl ether, yield 63%. Mp = 190.0 °C.

***N*-(3-Hydroxycarbamoylbenzyl)-1,2,4,9-tetrahydro-3-thia-9-azafluorene-3,3-dioxide 3c.** ^{1}**H NMR** (400 MHz, d_6-DMSO): δ 3.24 and 3.51 (2 × t, J = 6.0 Hz, 2 × 2H), 4.50 (s, 2H), 5.47 (s, 2H), 7.06–7.11 (m, 2H), 7.14–7.18 (m, 1H), 7.37 (t, J = 7.9 Hz, 1H), 7.48–7.51 (m, 2H), 7.59–7.61 (m, 2H), 9.04 (bs, 1H), 11.22 (bs, 1H). ^{13}**C NMR** (100.6 MHz, d_6-DMSO): δ 22.4, 46.2, 46.7, 48.4, 102.7, 110.4, 118.2, 120.0, 122.4, 126.0, 126.1, 126.6, 129.3, 129.5, 131.5, 133.8, 137.1, 138.9, 164.5. **MS** (70 eV): m/z (%) = 371 ([M + 1]$^+$, 95). **HRMS** (ESI) m/z for $C_{19}H_{19}N_2O_4S$ [M + H]$^+$ calcd 371.1060, found 371.1066. Yellow powder. Crystallization from diethyl ether, yield 32%. Mp = 229.5 °C.

***N*-(3-Hydroxycarbamoylbenzyl)-6-fluoro-1,2,4,9-tetrahydro-3-thia-9-azafluorene-3,3-dioxide 3d.** ^{1}**H NMR** (400 MHz, d_6-DMSO): δ 3.23 and 3.50 (2 × t, J = 5.9 Hz, 2 × 2H), 4.48 (s, 2H), 5.47 (s, 2H), 7.00 (t × d, J = 9.1, 2.5 Hz, 1H), 7.08 (d, J = 7.5 Hz, 1H), 7.32 (d × d, J = 9.7, 2.5 Hz, 1H), 7.34–7.38 (m, 1H), 7.50 (d × d, J = 9.1, 4.3 Hz, 1H), 7.58 (s, 1H), 7.61 (d, J = 7.5 Hz, 1H), 9.05 (bs, 1H), 11.21 (bs, 1H). ^{13}**C NMR** (100.6 MHz, d_6-DMSO): δ 22.5, 46.4, 46.6, 48.3, 102.9 (d, J = 4.6 Hz), 103.4 (d, J = 24.0 Hz), 110.3 (d, J = 26.1 Hz), 111.5 (d, J = 9.5 Hz), 125.9, 126.1, 126.9 (d, J = 10.2 Hz), 129.2, 129.4, 133.5, 133.7, 133.8, 138.6, 157.7 (d, J = 232.9 Hz), 164.3. ^{19}**F NMR** (376.5 MHz, d_6-DMSO): δ (−124.15)–(−124.09) (m). **MS** (70 eV): m/z (%) = 389 ([M + 1]$^+$, 100). **HRMS** (ESI) m/z for $C_{19}H_{18}FN_2O_4S$ [M + H]$^+$ calcd 389.0966, found 389.0967. White powder. Crystallization from EtOH, yield 5%. Mp = 237.0 °C.

***N*-(3-Hydroxycarbamoylbenzyl)-6-phenyl-1,2,4,9-tetrahydro-3-thia-9-azafluorene-3,3-dioxide 3e.** ^{1}**H NMR** (400 MHz, d_6-DMSO): δ 3.25 and 3.52 (2 × t, J = 5.8 Hz, 2 × 2H), 4.57 (s, 2H), 5.49 (s, 2H), 7.10 (d, J = 7.4 Hz, 1H), 7.30–7.36 (m, 2H), 7.44–7.48 (m, 3H), 7.57 (d, J = 8.6 Hz, 1H), 7.61–7.63 (m, 2H), 7.70 (d, J = 7.2 Hz, 2H), 7.81 (s, 1H) 9.02 (bs, 1H), 11.17 (bs, 1H). ^{13}**C NMR** (100.6 MHz, d_6-DMSO): δ 22.5, 46.4, 46.7, 48.5, 103.2, 110.8, 116.5, 121.6, 125.7, 126.0, 126.9, 127.1, 127.2, 129.1, 129.2, 129.3, 132.3, 132.5, 134.2, 136.7, 138.6, 141.8, 164.0. **MS** (70 eV): m/z (%) 447 ([M + 1]$^+$, 85). **HRMS** (ESI) m/z for $C_{25}H_{23}N_2O_4S$ [M + H]$^+$ calcd 447.1373, found 447.1361. White powder. Crystallization from CH_2Cl_2, yield 63%. Mp = 214.0 °C.

***N*-(3-Hydroxycarbamoylbenzyl)-2,3-dihydrothieno[3,2-*b*]indole-1,1-dioxide 3f.** ^{1}**H NMR** (400 MHz, d_6-DMSO): δ 3.47 and 3.96 (2 × t, J = 6.5 Hz, 2 × 2H), 5.50 (s, 2H), 7.22–7.34 (m, 3H), 7.43 (t, J = 7.9 Hz, 1H), 7.58–7.61 (m, 2H), 7.65–7.66 (m, 2H), 9.04 (bs, 1H), 11.24 (bs, 1H). ^{13}**C NMR** (100.6 MHz, d_6-DMSO): δ 21.0, 47.1, 57.4, 112.3, 116.1, 118.7, 119.3, 122.5, 123.9, 126.3, 126.6, 129.4, 130.3, 133.8, 137.4, 141.0, 148.5, 164.3. **MS** (70 eV): m/z (%) = 357 ([M + 1]$^+$, 100). **HRMS** (ESI) m/z for $C_{18}H_{17}N_2O_4S$ [M + H]$^+$ calcd 357.0904, found 357.0907. White powder. Crystallisation from ethanol, yield 25%. Mp = 236.5 °C.

***N*-(3-Hydroxycarbamoylbenzyl)-7-fluoro-2,3-dihydrothieno[3,2-*b*]indole-1,1-dioxide 3g.** ^{1}**H NMR** (400 MHz, d_6-DMSO): δ 3.47 and 3.96 (2 × t, J = 6.5 Hz, 2 × 2H), 5.51 (s, 2H), 7.17 (t × d, J = 9.2, 2.5 Hz, 1H), 7.33 (d, J = 7.8 Hz, 1H), 7.38–7.45 (m, 2H), 7.61 (d × d, J = 9.2, 4.3 Hz, 1H), 7.65–7.67 (m, 2H), 9.04 (bs, 1H), 11.23 (bs, 1H). ^{13}**C NMR** (100.6 MHz, d_6-DMSO): δ 21.1, 47.3, 57.3, 104.2 (d, J = 25.4 Hz), 112.0 (d, J = 25.8 Hz), 113.8 (d, J = 9.7 Hz), 116.1 (d, J = 4.4 Hz), 119.5 (d, J = 11.2 Hz), 126.3, 126.7, 129.5, 130.3, 133.9, 137.2, 137.6, 150.1, 158.7 (d, J = 236.6 Hz), 164.3. ^{19}**F NMR** (376.5 MHz, d_6-DMSO): δ (−120.64)–(−120.58) (m). **MS** (70 eV): m/z (%) = 375 ([M + 1]$^+$, 87). **HRMS** (ESI) m/z for $C_{18}H_{16}FN_2O_4S$ [M + H]$^+$ calcd 375.0809, found 375.0810. White powder. Crystallisation from diethyl ether, yield 40%. Mp > 260.0 °C.

***N*-(3-Hydroxycarbamoylbenzyl)-7-bromo-2,3-dihydrothieno[3,2-*b*]indole-1-oxide 3h.** ^{1}**H NMR** (400 MHz, d_6-DMSO): δ 3.24–3.31 (m, 1H), 3.36–3.43 (m, 1H), 3.57–3.64 (m, 1H), 4.00–4.07 (m, 1H), 5.51 and 5.57 (2 × d, J = 16.3 Hz, 2 × 1H), 7.31 (d, J = 7.9 Hz, 1H), 7.38 (d × d, J = 8.8, 1.9 Hz, 1H), 7.42 (t, J = 7.9 Hz, 1H), 7.56 (d, J = 8.8 Hz, 1H), 7.64–7.66 (m, 2H), 7.90 (d, J = 1.9 Hz, 1H), 9.04 (bs, 1H), 11.23 (bs, 1H). ^{13}**C NMR** (100.6 MHz, d_6-DMSO): δ 23.9, 48.5, 58.5, 114.1, 114.6, 120.4, 121.2, 124.4, 125.5, 126.3, 126.6, 129.4, 130.2, 133.9, 137.4, 140.2, 154.6, 166.3. **MS** (70 eV): m/z (%) 419/21 ([M + 1]$^+$, 100). **HRMS** (ESI) m/z for $C_{18}H_{16}BrN_2O_3S$ [M + H]$^+$ calcd 419.0060, found 419.0056. White powder. Recrystallization from CH_2Cl_2, yield 70%. Mp = 218.5 °C.

***N*-(4-Hydroxycarbamoylbenzyl)-1,2,4,9-tetrahydro-3-thia-9-azafluorene-3-oxide 3i.** **^{1}H NMR** (400 MHz, d_6-DMSO): δ 3.02–3.16 (m, 3H), 3.32–3.38 (m, 1H), 4.03 and 4.22 (2 × d, J = 15.2 Hz, 2 × 1H), 5.48 (s, 2H), 7.04–7.15 (m, 4H), 7.44 (d, J = 8.1 Hz, 1H), 7.51 (d, J = 7.6 Hz, 1H), 7.66 (d, J = 8.2 Hz, 2H), 9.00 (bs, 1H), 11.14 (bs, 1H). **^{13}C NMR** (100.6 MHz, d_6-DMSO): δ 16.6, 43.9, 44.8, 45.9, 99.7, 110.1, 118.1, 119.8, 122.0, 126.8, 127.6, 127.7, 132.3, 133.2, 136.7, 141.7, 164.4. **MS** (70 eV): m/z (%) = 355 ([M + 1]$^+$, 100). **HRMS** (ESI) m/z for $C_{19}H_{19}N_2O_3S$ [M + H]$^+$ calcd 355.1111, found 355.1112. White powder. Crystallisation from EtOH, yield 13%. Mp = 258.5 °C.

***N*-(4-Hydroxycarbamoylbenzyl)-6-fluoro-1,2,4,9-tetrahydro-3-thia-9-azafluorene-3-oxide 3j.** **^{1}H NMR** (400 MHz, d_6-DMSO): δ 3.01–3.15 (m, 3H), 3.28–3.38 (m, 1H), 4.02 and 4.17 (2 × d, J = 15.6 Hz, 2 × 1H), 5.44 (s, 2H), 6.95 (t × d, J = 9.0, 2.5 Hz, 1H), 7.09 (d, J = 8.2 Hz, 2H), 7.32 (d × d, J = 9.7, 2.5 Hz, 1H), 7.45 (d × d, J = 9.0, 4.3 Hz, 1H), 7.67 (d, J = 8.2 Hz, 2H), 9.00 (bs, 1H), 11.15 (bs, 1H). **^{13}C NMR** (100.6 MHz, d_6-DMSO): δ 16.5, 43.7, 44.6, 46.0, 100.0 (d, J = 4.3 Hz), 103.3 (d, J = 23.7 Hz), 109.8 (d, J = 26.1 Hz), 111.2 (d, J = 9.7 Hz), 126.8, 127.8, 128.0 (d, J = 10.0 Hz), 132.4, 133.3, 135.3, 141.5, 157.7 (d, J = 231.9 Hz), 164.4. **^{19}F NMR** (376.5 MHz, d_6-DMSO): δ (−124.45)–(−124.39) (m). **MS** (70 eV): m/z (%) = 373 ([M + 1]$^+$, 100). **HRMS** (ESI) m/z for $C_{19}H_{18}FN_2O_3S$ [M + H]$^+$ calcd 373.1017, found 373.1014. White powder. Crystallisation from EtOH, yield 28%. Mp = 244.5 °C.

***N*-(4-Hydroxycarbamoylbenzyl)-6-bromo-1,2,4,9-tetrahydro-3-thia-9-azafluorene-3,3-dioxide 3k.** **^{1}H NMR** (400 MHz, d_6-DMSO): δ 3.22 and 3.51 (2 × t, J = 5.9 Hz, 2 × 2H), 4.51 (s, 2H), 5.50 (s, 2H), 7.07 (d, J = 8.2 Hz, 2H), 7.27 (d × d, J = 8.7, 1.7 Hz, 1H), 7.47 (d, J = 8.7 Hz, 1H), 7.67 (d, J = 8.2 Hz, 2H), 7.75 (d, J = 1.7 Hz, 1H), 9.01 (bs, 1H), 11.16 (bs, 1H). **^{13}C NMR** (100.6 MHz, d_6-DMSO): δ 22.4, 46.2, 46.5, 48.2, 102.7, 112.5, 112.7, 120.8, 124.8, 126.8, 127.8, 128.3, 132.5, 133.3, 135.8, 141.2, 164.3. MS (70 eV): m/z (%) 449/51 ([M + 1]$^+$, 5). HRMS (ESI) m/z for $C_{19}H_{18}BrN_2O_4S$ [M + H]$^+$ calcd 449.0165, found 449.0148. White powder. Crystallisation from CH_2Cl_2, yield 70%. Mp = 230.0 °C.

***N*-(4-Hydroxycarbamoylbenzyl)-2,3-dihydrothieno[3,2-*b*]indole-1,1-dioxide 3l.** **^{1}H NMR** (400 MHz, d_6-DMSO): δ 3.46 and 3.96 (2 × t, J = 6,3 Hz, 2 × 2H), 5.51 (2H, s), 7.22–7.30 (m, 4H), 7.56–7.61 (m, 2H), 7.71 (d, J = 8.2 Hz, 2H), 9.03 (bs, 1H), 11.17 (bs, 1H). **^{13}C NMR** (100.6 MHz, d_6-DMSO): δ 20.9, 47.0, 57.4, 112.3, 116.1, 118.7, 119.3, 122.5, 123.9, 127.5, 127.9, 132.7, 140.1, 140.9, 148.5, 164.2. **MS** (70 eV): m/z (%) = 357 ([M + 1]$^+$, 33), 374 ([M + NH_4^+], 100). **HRMS** (ESI) m/z for $C_{18}H_{17}N_2O_4S$ [M + H]$^+$ calcd 357.0904, found 357.0900. White powder. Crystallisation from EtOH, yield 25%. Mp = 198.0 °C.

***N*-(4-Hydroxycarbamoylbenzyl)-7-fluoro-2,3-dihydrothieno[3,2-*b*]indole-1,1-dioxide 3m.** **^{1}H NMR** (400 MHz, d_6-DMSO): δ 3.47 and 3.96 (2 × t, J = 6.5 Hz, 2 × 2H), 5.51 (s, 2H), 7.16 (t × d, J = 9.2, 2.5 Hz, 1H), 7.29 (d, J = 8.2 Hz, 2H), 7.40 (d × d, J = 9.1, 2.5 Hz, 1H), 7.60 (d × d, J = 9.2, 4.3 Hz, 1H), 7.72 (d, J = 8.2 Hz, 2H), 9.03 (bs, 1H), 11.19 (bs, 1H). **^{13}C NMR** (100.6 MHz, d_6-DMSO): δ 21.0, 47.2, 57.3, 104.3 (d, J = 25.3 Hz), 112.0 (d, J = 26.2 Hz), 113.7 (d, J = 9.8 Hz), 116.2 (d, J = 5.3 Hz), 119.5 (d, J = 11.1 Hz), 127.5, 127.9, 132.8, 137.6, 139.9, 150.1, 158.7 (d, J = 235.5 Hz), 164.2. **^{19}F NMR** (376.5 MHz, d_6-DMSO): δ (−120.60)–(−120.54) (m). **MS** (70 eV): m/z (%) = 392 ([M + NH_4^+], 100). **HRMS** (ESI) m/z for $C_{18}H_{19}FN_3O_4S$ [M + NH_4^+] calcd 392.1075, found 392.1075. White powder. Crystallisation from diethyl ether, yield 5%. Mp = 240.5 °C.

Docking studies (performed at the Centre for Industrial Biotechnology and Biocatalysis)

All manipulations were performed with the molecular modelling program YASARA and the YASARA/WHATIF twinset,[16] and the figure was created with PyMol v1.3.[17] The HDAC6 sequence was obtained from the UniProt database (http://www.uniprot.org, UniProt entry Q9UBN7). To increase the accuracy of the model, the sequence was limited to the major functional domain of HDAC6 (Gly482–Gly800). Possible templates were identified by running 3 PSI-BLAST iterations to extract a position specific scoring matrix (PSSM) from UniRef90, and then searching the PDB for a match. To aid the alignment of the HDAC6 sequence and templates, and the modelling of the loops, a secondary structure prediction was performed, followed by multiple sequence alignments. All side chains were ionised or kept neutral according to their predicted pK_a values. Initial models were created from different templates (pdb entry 2VQW, 2VQQ and 3C10), each with several alignment variations and up to hundred conformations tried per loop. After the side-chains had been built, optimised and fine-tuned, all newly modelled parts were subjected to a combined steepest descent and simulated annealing minimisation, *i.e.* the backbone atoms of aligned residues were kept fixed to preserve the folding, followed by a full unrestrained simulated annealing minimisation for the entire model. The final model was obtained as a hybrid model of the best parts of the initial models, and checked once more for anomalies like incorrect configurations or colliding side chains. Furthermore, it was structurally aligned with known HDAC crystal structures to check if the chelating residues and the zinc atom were arranged correctly. The HDAC inhibitor structures were created with YASARA Structure and energy minimised with the AMBER03 force field.[18] The grid box used for docking had a dimension of 25 × 25 × 25 angstrom, and comprised the entire catalytic cavity including the zinc ion and the outer surface of the active site entrance. Docking was performed with AutoDock VINA[19] and default parameters. Ligands were allowed to freely rotate during docking. The first conformer from the cluster that has its zinc binding group in the vicinity of the zinc ion, was selected as the binding mode for analysis.

Enzyme inhibition assay (performed by Eurofins Cerep Panlabs)

In vitro determination of IC_{50}-values by using human recombinant HDAC1-11 and fluorogenic HDAC substrate.[20] For more details, see ESI.†

Western blots (performed at the Laboratory of Neurobiology and Vesalius Research Center, VIB)

Values represent the normalized ratio acetyl α-tubulin/α-tubulin and acetyl histone 3/histone 4 against Tubastatin A (Tub A) in an established neuronal cell line (Neuro-2a cells: ATCC N° CCL-131).

Cell culture

Mouse neuroblastoma (Neuro-2a) cells were grown in a 1 : 1 mix of D-MEM (Dulbecco's Modified Eagle Medium) and F12 medium supplemented with glutamax (Life Technologies), 100 μg per ml streptomycin, 100 U per ml penicillin (Life Technologies), 10% fetal calf serum (Greiner Bio-one), 1% non-essential amino acids (Life Technologies) and 1.6% $NaHCO_3$ (Life Technologies) at 37 °C and 7.5% CO_2. To split the cells, cells were washed with Versene (Life Technologies) and dissociated with 0.05% Trypsine-EDTA (Life Technologies). The Neuro-2a cells were treated overnight at 37 °C with dosages ranging from 10 nM up to 1 μM of either Tubastatin A (Asclepia, Destelbergen, Belgium) or the candidate HDAC6 inhibitors, and the effect on the acetylation level of α-tubulin is determined by using western blot. For more details, see ESI.†

Western blot

For sodium dodecyl sulfate-polyacrylamide gel electrophoresis (SDS-PAGE) analysis, treated cells were collected using the EpiQuik Total Histone Extraction Kit (EpiGentek) according to manufacturer's instructions. Protein concentrations were determined using microBCA kit (Thermo Fisher Scientific Inc., Pittsburgh, PA, USA) according to manufacturer's instructions. Before resolving the samples on a 12% SDS-PAGE gel, samples containing equal amounts of protein were supplemented with reducing sample buffer (Thermo Scientific) and boiled at 95 °C for 5 min. After electrophoresis, the proteins were transferred to a polyvinylidene difluoride (PVDF) membrane (Millipore Corp.). The non-specific binding was blocked by incubation of the membrane in 5% bovine serum albumin (BSA), diluted in Tris Buffered Saline Tween (TBST, 50 mM TRIS, 150 mM NaCl, 0.1% Tween-20 (Applichem, Darmstadt, Germany) overnight followed by incubation with primary antibodies during one hour. The antibodies, diluted in TBS-T, were directed against α-tubulin (Sigma-Aldrich, T6199, 1/5000, 1h), against acetylated α-tubulin (Sigma-Aldrich, T6793, 1/5000, 1h), against glyceraldehyde 3-phosphate dehydrogenase (GAPDH, Life Technologies, AM4300, 1/5000, 1h), against histone H3 acetyl k9-k14 (Cell Signaling, 9677L, 1/500, 1h) and against histone 4 (Abcam, ab10158, 1/500, 1h). The secondary antibodies, coupled to alkaline phosphatase (anti-mouse or anti-rabbit, Sigma-Aldrich, 1/5000, 1h) were used. Blots were visualized by adding the ECF substrate (Enhanced Chemical Fluorescence, GE Healthcare, Uppsala, Sweden) and imaged with the ImageQuant_LAS 4000. A mild reblotting buffer (Millipore) was applied to strip the blots. ImageQuant TL version 7.0-software was used to quantify the blots.

Ames fluctuation assay (performed by Eurofins Cerep Panlabs)

Wells that displayed bacteria growth due to the reversion of the histidine mutation (as judged by the ratio of OD430/OD570 being greater than 1.0) are counted and recorded as positive counts. The significance of the positive counts between the treatment (in the presence of test compound) and the control (in the absence of test compound) are calculated using the one-tailed Fisher's exact test. Three significance levels are reported as follows: weak positive, if $0.01 \leq p < 0.05$, denoted as "+", strong positive, if $0.001 \leq p < 0.01$, denoted as "++", very strong positive, if $p < 0.001$, denoted as "+++". For more details, see ESI.†

Acknowledgements

This research was supported by the Ghent University Special Research Fund (BOF) and the Ghent University Industrial Research Fund (IOF, F2014 IOF StarTT 029). V. Benoy, W. Haeck and L. Van Den Bosch are supported by grants from the Research Foundation – Flanders (FWO-Vlaanderen), the University of Leuven, the Belgian government (Interuniversity Attraction Poles of the Belgian Federal Science Policy Office), the Association Belge contre les Maladies neuro-Musculaires (ABMM), the ALS Association (ALSA), the ALS Therapy Alliance, the Muscular Dystrophy Association (MDA), and the European Community's Health Seventh Framework Programme (FP7/2007–2013 under grant agreement 259867). V. Benoy is supported by the Agency for Innovation by Science and Technology in Flanders (IWT-Vlaanderen). S. J. Shuttleworth and S. Kerry (Karus Therapeutics Ltd) are greatly acknowledged for their contribution concerning ADMET.

References

1 C. H. Arrowsmith, C. Bountra, P. V. Fish, K. Lee and M. Schapira, *Nat. Rev. Drug Discovery*, 2012, **11**, 384–400.
2 A. J. M. De Ruijter, A. H. Van Gennip, H. N. Caron, S. Kemp and A. B. P. Van Kuilenburg, *Biochem. J.*, 2003, **370**, 737–749.
3 (*a*) C. Scholz, B. T. Weinert, S. A. Wagner, P. Beli, Y. Miyake, J. Qi, L. J. Jensen, W. Streicher, A. R. McCarthy, N. J. Westwood, S. Lain, J. Cox, P. Matthias, M. Mann, J. E. Bradner and C. Choudhary, *Nat. Biotechnol.*, 2015, **33**, 415–423; (*b*) X.-J. Yang and E. Seto, *Nat. Rev. Mol. Cell Biol.*, 2008, **9**, 206–218; (*c*) G. Giannini, W. Cabri, C. Fattorusso and M. Rodriquez, *Future Med. Chem.*, 2012, **4**, 1439–1460.
4 I. V. Gregoretti, Y. M. Lee and H. V. Goodson, *J. Mol. Biol.*, 2004, **338**, 17–31.
5 L. Van Helleputte, V. Benoy and L. Van Den Bosch, *Res. Rep. Biol.*, 2014, **5**, 1–13.
6 (*a*) G. I. Aldana-Masangkay and K. M. Sakamoto, *J. Biomed. Biotechnol.*, 2011, 875824; (*b*) S. Dallavalle, C. Pisano and F. Zunino, *Biochem. Pharmacol.*, 2012, **84**, 756–765.

7 (*a*) M. R. Shakespear, M. A. Halili, K. M. Irvine, D. P. Fairlie and M. J. Sweet, *Trends Immunol.*, 2011, **32**, 335–343; (*b*) J. H. Kalin and J. A. Bergman, *J. Med. Chem.*, 2013, **56**, 6297–6313.

8 (*a*) K. V. Butler, J. Kalin, C. Brochier, G. Vistoli, B. Langley and A. P. Kozikowski, *J. Am. Chem. Soc.*, 2010, **132**, 10842–10846; (*b*) K. V. Woan, M. Lienlaf, P. Perez-Villaroel, C. Lee, F. Cheng, T. Knox, D. M. Woods, K. Barrios, J. Powers, E. Sahakian, H. W. Wang, J. Canales, D. Marante, K. S. Smalley, J. Bergman, E. Seto, A. Kozikowski, J. Pinilla-Ibarz, A. Sarnaik, E. Celis, J. Weber, E. M. Sotomayor and A. Villagra, *Mol. Oncol.*, 2015, **9**, 1447–1457; (*c*) J. H. Kalin, K. V. Butler, T. Akimova, W. W. Hancock and A. P. Kozikowski, *J. Med. Chem.*, 2012, **55**, 639–651.

9 R. De Vreese, T. Verhaeghe, T. Desmet and M. D'hooghe, *Chem. Commun.*, 2013, **49**, 3775–3777.

10 F. Thaler and C. Mercurio, *ChemMedChem*, 2014, **9**, 523–536.

11 D. E. Olson, F. F. Wagner, T. Kaya, J. P. Gale, N. Aidoud, E. L. Davoine, F. Lazzaro, M. Weiwer, Y. L. Zhang and E. B. Holson, *J. Med. Chem.*, 2013, **56**, 4816–4820.

12 A. Sudhakara, H. Jayadevappa, H. N. H. Kumar and K. M. Mahadevan, *Lett. Org. Chem.*, 2009, **6**, 159–164.

13 M. V. Kozlov, A. A. Kleymenova, K. A. Konduktorov and S. N. Kochetkov, *Russ. J. Bioorg. Chem.*, 2013, **39**, 102–105.

14 (*a*) C. Y. Wang, *Mutat. Res.*, 1977, **56**, 7–12; (*b*) P. L. Skipper, S. R. Tannenbaum, W. G. Thilly, E. E. Furth and W. W. Bishop, *Cancer Res.*, 1980, **40**, 4704–4708.

15 For a full account on the nonclinical safety assessment of Vorinostat, see: S. Galloway, A. Lagrutta, M. Armstrong, T. Miller, V. M. Richon and P. A. Andrews, *Int. J. Toxicol.*, 2010, **29**, 3–19.

16 (*a*) E. Krieger, G. Koraimann and G. Vriend, *Proteins*, 2002, **47**, 393–402; (*b*) G. Vriend, *J. Mol. Graphics*, 1990, **8**, 52–56.

17 L. Schrodinger, 2010.

18 Y. Duan, C. Wu, S. Chowdhury, M. C. Lee, G. M. Xiong, W. Zhang, R. Yang, P. Cieplak, R. Luo, T. Lee, J. Caldwell, J. M. Wang and P. Kollman, *J. Comput. Chem.*, 2003, **24**, 1999–2012.

19 O. Trott and A. J. Olson, *J. Comput. Chem.*, 2010, **31**, 455–461.

20 B. D. Strahl and C. D. Allis, *Nature*, 2000, **403**, 41–45.